Design of a flexible hybrid powertrain using a 48V-battery and a supercapacitor for ultra-light urban vehicles

Ouafae El Ganaoui-Mourlan, El-Hadj Miliani, Daniel Carlos da Silva, Matthieu Couillandeau, Charlie Gonod, Guillaume Miller

Design of a flexible hybrid powertrain using a 48V-battery and a supercapacitor for ultra-light urban vehicles

Abstract

Global warming has put the transport sector, a major contributor of CO_2 emissions, under high pressure to improve efficiency. In this context, ultra-light vehicles weighting less than 500 kg, as well as hybrid powertrains, are nowadays seen as promising development trends. The design process of the powertrain of a vehicle combining the advantages of the two concepts is presented in this paper. Through a performance study based on a simple MATLAB model, and mathematical simulation, a proposal is made. A powertrain using a battery and supercapacitor 48V dual power source network, two electric motors and clutches to switch between conventional, parallel, series and full electric modes proves to be an interesting system in terms of performance and costs. A simulation study conducted on a scenario with different outcome possibilities showed that high modularity of the system allows to achieve fuel efficiencies equivalent to approximately 3 l/100 km on the Artemis cycle. Finally, integration, packaging and cost are considered and some hints for further powertrain efficiency improvements are presented.

Introduction

City congestion and reduction of CO_2 emissions are both major preoccupations that governments are nowadays striving to tackle. For this purpose, new ways of urban mobility are coming up, such as car, bike-, or even scooter-sharing, and public transports networks are expending. However, commuters that live in remote suburban area are often bound to use their personal vehicle. For these kind of road users, no other mean that regular passenger cars are available. Indeed, a study conducted by the American Federal Highway Administration [1] calculated an average occupancy of the typical American car to be 1.7. Another European study expressed the same figure for the Old Continent [2]. Given that the average mass of a car can easily range from 1200 to 1800kg, it is not surprising that new solutions are being investigated.

In this context, a new type of vehicle has emerged. At the crossroad between small car (e.g. M1 segment Smart) and cart or trike, these light electric vehicles, symbolised by the Renault Twizy, are subject to more and more research from car industry stakeholders. In practice, these vehicles can either be 3 or 4 wheelers, requiring a regular car driving license in most countries.

Besides, this category of vehicle comprises several features that justify the interest they are sparking:

- Light weight: use of a smaller powertrain, meaning a reduced fuel consumption.
- Small size and agility in traffic
- Cost efficiency: (including utilization cost and maintenance cost)
- Highway-driving ability

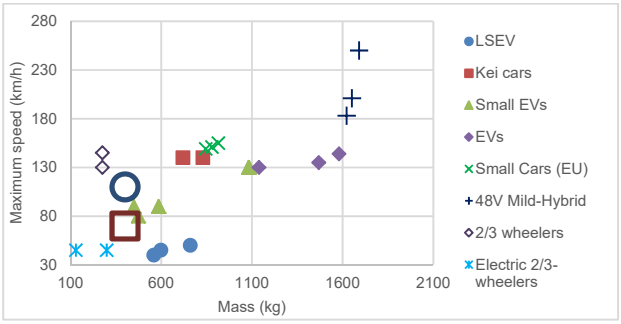

Figure 1: market study of some vehicle categories (internet study: https://www.automobile-propre.com/)

As shown in Figure 1, the maximum vehicle speed is somehow dependent on its mass. The performance of the car defined in this study should be set somewhere between small EVs (type Twizy) and 3 wheelers, where no closed cabin vehicle exists yet. Besides power, the range is a limitation of EVs, especially when relatively high speeds are reached (extra-urban driving). To make up for these shortcomings, a hybrid powertrain could be an interesting solution.

However, the characteristic of the vehicle evoked previously make the implementation of a dual-energy powertrain challenging. The room available for it is limited and the weight and cost should not be increased too much compared to a conventional powertrain, whilst keeping the same rated power.

In order to determine the best powertrain match for a vehicle of this nature, a critical analysis of the requirements and existing technologies will first be undertaken, in order to better understand the aim of the vehicle and to make first technical choices.

Then, a power requirement study followed by a comparison of the retained architectures will be performed. They will be based on simplified models running on given operating points corresponding to typical driving cases. Through this study, the one architecture for the full cycle (Artemis) simulation will be selected.

In a fourth part, the chosen architecture and its modelling will be presented. It will highlight the vehicle performance in terms of consumption on some driving patterns.

Then, detailed technical choices will be described, and packaging and cost considerations will be introduced.

Finally, a description of some innovative ways to make, on the medium term, the vehicle more efficient will be provided, to look a bit further into ways to enhance the packaging/cost performance of the retained solution.

Target vehicle definition

In this work, the aim is to study a vehicle, mainly designed for urban use, that fulfill the following requirements and constraints:

(i) The car should be able to cover daily travels as an electric vehicle
a. Short electric range (30 km)
b. Two seats
c. Low maximum speed (70 km/h, rarely excessed in urban environment)
(ii) The car should not be strictly limited to daily travels
a. Reasonable overall range in hybrid mode (300km)
b. High maximum speed in hybrid mode (110km/h)
(iii) The car should be able to accelerate from 0 to 100 km/h in less than 13 s (safety)
(iv) The car should have a cost as low as possible
a. Low vehicle price
b. Low fuel consumption (high efficiency)
c. Low TCO (e.g. long battery life).
(v) The car should have a very low environmental footprint, as potential customers are likely to be sensitive to these questions.

Table 1 sums up the main characteristics of the vehicle described above.

Table 1: target vehicle main characteristics

Dimensions		Performances		Range	
Length (m)	2,5	$v_{max\ i_{ZE}}$ (km/h)	70	ZE range (km)	30
Width (m)	0,9	v_{maxi} (km/h)	110	Total (km)	300
Mass (kg)	400	0-100 (s)	13		

Proposed powertrain architectures

Following the previously described analysis of the requirements and main specifications of the vehicle, some preliminary choices have been made, and some constraints identified.

In order to achieve performance and efficiency specifications (i, ii & iv.c), **a two-motor solution** has been chosen. This allows an increased modularity and flexibility and avoids very high currents in the machine during peak power, hence helping to reduce the size of the motor. Easy implementation and high efficiency push for a parallel architecture, but some aspects of series hybridisation such as EV feeling and independence between wheels and engine operating points could be very interesting too, especially in slow city cycles, where the engine operates generally at low efficiency. Because clutches are simple to control compared to epicyclic gears, a compound architecture is preferred to a split system.

Figure 2, Figure 3 and Figure 4 present the three architectures that are compared later in this paper on the basis of their efficiencies. Using two clutches, they allow to switch from parallel to series mode. To avoid confusion, the P1* label will refer to the closest MG from the engine, even though it is, strictly speaking, a P2 motor.

In the P1*/P2 architecture (Figure 2), the rotation speed of the two electric machines are directly linked to that of the engine, whereas in P1*/P3 (Figure 3), the manual transmission decouples the two speeds.

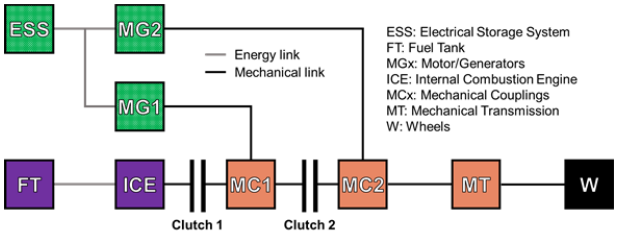

Figure 2: P1*/P2 architecture

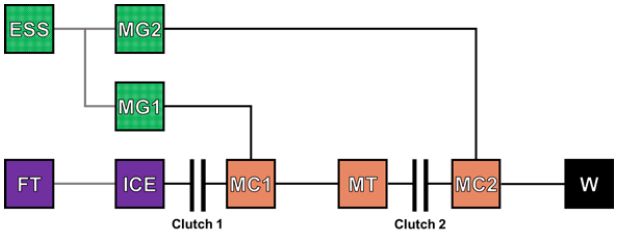

Figure 3: P1*/P3 architecture

In the P1*/P4 architecture (Figure 4), the two axles of the car may be equipped with a propulsion system. This could be interesting for packaging reasons (the volume of the powertrain is distributed between front and rear axles), allows to choose an appropriate final drive dedicated to the MG2, and could offer some advantages in drivability.

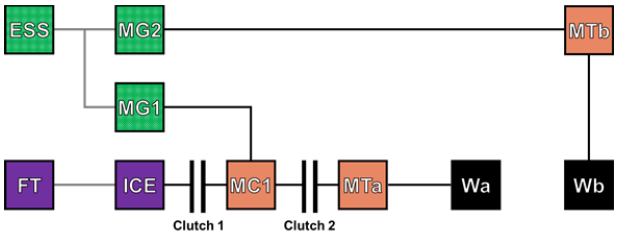

Figure 4: P1*/P4 architecture

To help reducing the fuel consumption, a **Stop and Start system** is implemented, as it is already the case on a high number of cars. This comes with a constraint linked to post-treatment systems, which prevents the engine to stop until 30 seconds after the last start.

As emphasised by numerous authors (J. Mortal [3], M. Forissier [4]), a **48V solution** could lead to a low-cost system (specification iv), while still being able to power the car. Another way of reducing the cost is the choice of a low power density battery with **supercapacitors** handling the peak power demands. In order to avoid the use of another starter-generator, one of the two motors is used to crank the engine.

Evaluation of the architecture performances

Power requirements

In order to determine the power that the powertrain must be able to deliver, two requirements are imposed. The vehicle must be able to accelerate from 0 to 100km/h in 13 seconds, and follow the Artemis driving cycle, limited at 110km/h (cf. target vehicle requirements, Table 1).

Vehicle model and assumptions

The vehicle motion is derived from the balance of the forces acting on it. These forces are the following: aerodynamic drag F_{aero}, rolling resistance F_{roll}, slope force F_{slope}, inertia force $F_{inertia}$, and traction force F_{trac}. Calculation of the traction force thanks to Equation 1 permits to derive the required power to fulfil the desired acceleration.

$$F_{trac} = F_{inertia} + F_{aero} + F_{roll} + F_{slope} \qquad (1)$$

The calculation of these different forces requires some assumptions on the vehicle characteristics. The unladen mass of the vehicle is 400 kg. The choice was made in this study to size the powertrain so that the vehicle can carry two adults of 80 kg (560 kg in total), which makes it fit in the L5e/L7e category. In addition to that, a mass factor of 4% has been applied to this value, aiming to represent the inertia of the rotary part of the driveline. The drag and rolling resistance coefficients are set at 0.3 and 0.02 respectively. These values are in accordance with those presented in [5].

Simulation and results

0-100km/h acceleration: Different cases have been modelled. First, 0–100km/h acceleration, was studied. A speed profile was created, such that the maximum power is reached at high speed and is presented in Figure 5.

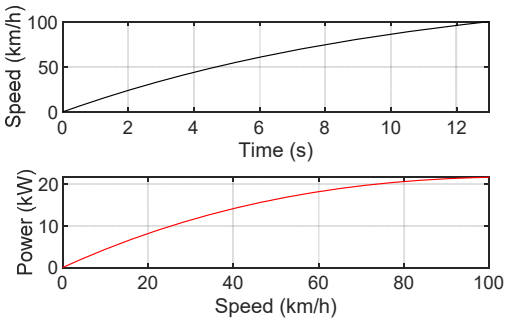

Figure 5: Power request for 0-100 kph acceleration criteria

At the end of the day, calculations showed that 22kW are required to fulfil the acceleration requirement defined previously.

Artemis cycle: The Artemis cycle, which is not used for official homologation tests, was the reference for analysis in this study. The most demanding part of the cycle is the last one, during the extra-urban phase, where the maximal power required is 24.5kW (Figure 6).

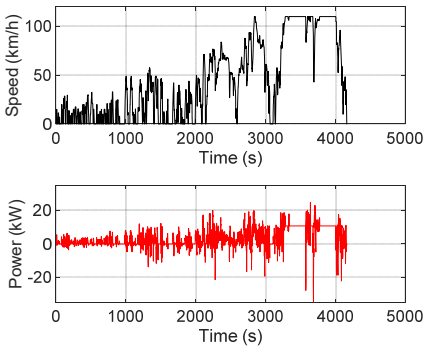

Figure 6: Power requirement on Artemis cycle

It is to notice that a significant amount of power is required to slow down the vehicle. That power can be partly recovered by regenerative braking. The rest of the energy is dissipated into the conventional brakes.

Sizing of the powertrain

In a hybrid architecture, the question of the power distribution between ICE and electric motors increases the complexity of the study. In order to be able to cruise on highways, the ICE has been dimensioned so it could at least cater for the power requirement at 110km/h stabilised, on a 5% positive slope. This power turns out to be close to 20kW, which is what a 0.3 L engine can deliver. When it comes to the electric powertrain, it must allow the car to maintain 70 km/h on a 5% slope, which corresponds to a value of 9.6 kW or 18.7 N.m at base speed (4900 rpm). That brings the total vehicle power to 30 kW which is sufficient to reach the requested performance for acceleration and Artemis profiles.

Regarding the battery capacity, the completion of 30 km in full electric mode should be possible. Simulation on the first 30 km of the Artemis cycle limited at 70 km/h without regeneration gives a battery capacity of 2.1 kWh.

These are pre-sized values which will be refined later on, taking into account various powertrain efficiencies and SoC limitations.

A comparative study on efficiencies

Each architecture presented on Figure 2, Figure 3 and Figure 4 have their advantages and drawbacks. In order to narrow down the options to one final architecture, these aspects have to be assessed. When comparing the architectures, two dimensions must be taken into account: first the efficiency and secondly the feasibility to evaluate the packaging, mass and cost.

As it is not possible to draw insights on the architectures efficiencies only by analysing the diagrams presented on Figure 2, Figure 3 and Figure 4, the Tool for the Assessment of Performances and Interest of Complex Architectures (TAPIoCA) was developed. This MATLAB script was conceived to assess the energy losses in the powertrain, focusing mainly on losses related to the operating points of ICE, MG1 and MG2; by using the provided machine efficiency maps.

The aim of TAPIoCA is to appraise the relative importance of component efficiencies on the architecture choice. Then, other

aspects related to integration are also studied leading to a final decision.

Notion of Degrees of Freedom

Hybrid powertrains are composed of at least to power sources. Therefore, while some power factors (speed/torques of components such as gear or motors), are fixed, other need to be managed by a so-called energy management system, in order to fully determine the powertrain energy flows [6]. Those power factors are called Degrees of Freedom (DoFs). Degrees of Freedom depend on the architecture and, for complex hybrids such as this case study, also on the operating mode.

Driving modes of the architectures

The proposed architectures have four different operating modes, i.e. Conventional, Hybrid parallel, Hybrid series and Zero-emissions Vehicle (ZEV) modes The effective differences between modes and their number of DoFs are presented on Table 2.

Table 2: Component state for each mode

	Conv.	Para.	Series	ZEV
ICE	on	on	on[(1)]	off
MG1	off	on	on	on
MG2	off	on	on	on
Clutch 1	closed	closed	closed	open
Clutch 2	closed	closed	open	closed
# of DoF	0	2	1[(1)]	1

(1) ICE supposed to run only in best efficiency area

Table 4 presents which parameters were taken as DoF. The spans of these parameters were discretised in 20 divisions between their boundary values. In addition to that, the value of the mechanical transmission ratio was varied from 0.5 to 15, with steps of 0.2, as a way of considering a range that does not limit the performance of an architecture. Finally, the options that result on impossible operating points of the machines were neglected.

Table 4: Degrees of Freedom for each mode

	DoF 1	DoF 2	MT Ratio
Conv.	-	-	0.5 – 15
Para.	T_{MG1}	T_{MG2}	0.5 – 15
Series	T_{ICE}	N_{ICE}[(1)]	-
ZEV	T_{MG2}	-	0.5 – 15

(1) Only the N_{ICE} with the highest ICE efficiency is considered

Power allocation

Even though the first study resulted in a total electric torque of 18.7 N.m and an engine with 0.3 L of displacement, the electric power must be allocated between the two electric machines. To maintain a low complexity for this first study, the electric power was equally split, resulting in a maximum torque of 9.35 N.m. A more detailed distribution is performed once the architecture is defined.

Concerning the battery power, the boundaries were chosen based on batteries dedicated to mild hybrid vehicles. Thus, the maximum power for discharge was taken as 11 kW and, for recharge, 14 kW [7].

Global efficiency

Equation 2 shows the calculation of the Global Efficiency parameter, η_{global}, which was used to perform the comparison between the results, where P_{wheels} is the power at wheels, $P_{electric}$ is the power provided by the electrical source and P_{fuel} is the power provided by the fuel. The Global Efficiency considers all the losses along the power path from the sources to the wheels. Thus, the script identifies

Table 3: Considered setpoints for TAPIoCA script

	1	2	3	4	5	6
Case	Urban driving – ZEV available	Urban driving – no battery	Battery charging	70 km/h Hybrid	70 km/h ZEV mode	Motorway driving
Vel.	30 km/h	30 km/h	30 km/h	70 km/h	70 km/h	110 km/h
$P_{batt,max}$	14 kW	0 kW	-600 W	770 W	4 kW	14 kW

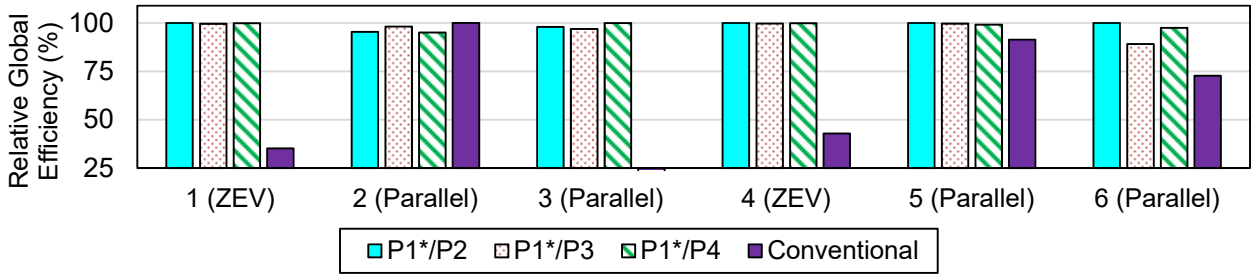

Figure 7: Architectures comparison using TAPIoCA on different setpoints

the DoF choice with the less amount of losses.

$$\eta_{global} = \frac{P_{wheels}}{P_{electric} + P_{fuel}} \quad (2)$$

However, the script will always try to find the result that uses the minimum possible the ICE, given that its efficiencies are around 2 to 3 times lower than the efficiencies of the used electric machine map. Ideally, this is indeed the best option in terms of efficient energy consumption. However, cases where the vehicle is obliged to use the energy from the fuel were created by limiting the maximum battery power. This considers that, in real operations, the powertrain will find itself in situations where the battery cannot be used or must be charged.

Considered setpoints

Considered setpoints to perform the comparison between architectures are presented on Table 3.

Results and justifications

After the calculation, the most relevant mode for each architecture was taken for each setpoint, i.e. the possible mode with the best overall global efficiency.

Figure 7 presents the global efficiency for all setpoints and for each architecture on the relevant mode, with respect to the higher value. Then, some conclusions can be drawn.

First, the series mode was not the most relevant mode for neither of the setpoints. This can be explained by the overdependency on the only propulsion source MG2. This can be improved by a deeper study on the ratios between the wheels and MG2.

Also, for some driving conditions, such as the one defined on setpoint 2, the conventional mode appears to be an interesting option to be considered.

Finally, not many differences can be seen between the three architectures. This leads to the final conclusion of the TAPIoCA script: the three architectures do not show any relevant advantages and drawbacks between themselves in terms of power losses, at least not without more complex calculations. Therefore, the architecture chosen for the rest of the work must be defined by integration and cost criteria.

Choice of architecture

Figure 7 shows very close results in terms of global efficiency, for the different architectures (except for P1*/P3 on setpoint 6). Therefore, the three architectures can be considered equivalent in terms of performance, as far as this study is concerned. Thus, the choice is made based on other criteria. As architecture P1*/P4 offers advantages in terms of packaging and allows to select a proper final drive ratio dedicated to the MG2, this architecture is chosen.

Modelling and optimisation

The vehicle architecture is described in Figure 8. At this stage of the project, different design choices are still to be made, such as the values of the final drives, the size of the battery, of the supercapacitor, the maximum total electric power and the allocation of this power between front and rear axle.

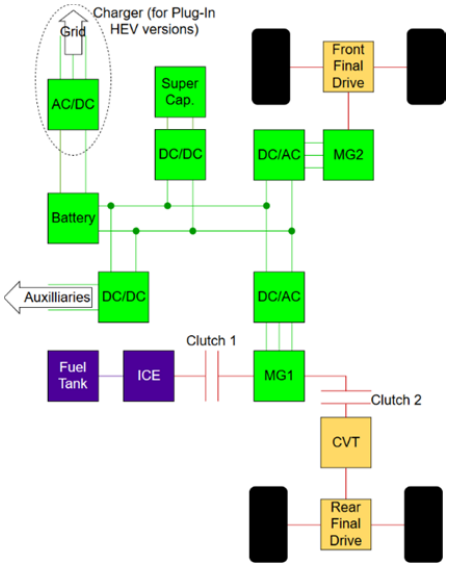

Figure 8: Detailed view of the P1*/P4 architecture

Description of the Developed Model

To implement the different design choices and draw conclusions on strategies, components sizing and final results, a Simulink model of the P1*/P4 architecture was developed. On the following sections, the theory behind the model, the steps of the study and the considered features are described.

Concept of backward and forward simulations

Different classes of models can be used to represent a hybrid architecture. The quasi-static models, as presented by [8], simplifies the system to the point of ignoring its dynamics, meaning that a change on the demand is taken into account instantly. It is also possible to categorise the quasi-static model in two types: the forward and the backward models [9]. The difference between the two is the agreement of the calculations order with the true physical causality on a real system.

Forward model: The forward model follows the physical causality: the input of the model is the same input as the real system.

Backward model: The backward model reverses the physical causality.

Simulink model layout

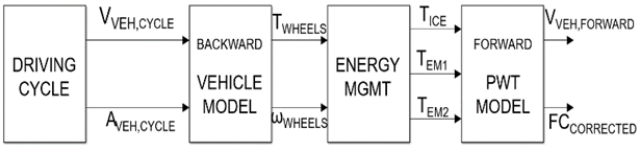

Figure 9: Layout of the model

Figure 9 presents a general layout of the developed model on

Simulink. In this model, both backward and forward approaches are applied. A driving cycle is used to compute the desired vehicle velocity and torque at wheels. The energy management strategy takes into account all the powertrain and driveline characteristics to set the optimal torque asked to the three mechanical power sources. Then, these torques are used in a forward model of the powertrain to verify whether the vehicle actually follows the input speed profile. It also calculates the corrected fuel consumption, which adds a conversion of the electric consumption to the genuine fuel consumption.

The same layout is then used for each driving mode: conventional, hybrid parallel, hybrid series and ZEV. Differences between modes are again explained in Table 2. Depending on the mode, the Energy Management block can also provide the gearbox ratio and a flag to indicate whether engine is on or off.

Description of the powertrain main models

Internal combustion engine: engine fuel consumption was computed using a reference map provided as an input of this study. A FMEP of 2 bars was considered. A Stop&Start control was also implemented as set out previously.

Electrical machines: Another map was used, and mirrored following the assumption that the electric machines have the same efficiency map whether they are working as motors or generators.

Battery: The battery considered is a cluster of battery cells, thus the way in which these cells are arranged defines the battery open circuit voltage and energy capacity. Also, the internal resistance of each cell, which is a function of SoC, was considered, allowing an estimation of the energy losses inside the battery (see *Hybrid energy storage* section later on).

Supercapacitors: Similarly to the battery they are arranged as a cluster of cells. However, their voltage decreases linearly, and boost converter is necessary to output a constant 48V voltage (see *Hybrid energy storage* section).

Energy Management

Inside the Energy Management block shown on Figure 9, the optimal energy distribution is performed by using the Pontryagin's Minimum Principle (PMP) with an offline approach, i.e. defining the strategy using a prescribed cycle [9]. It consists of a method to minimise the Hamiltonian (H), shown by Equation 3, which sums the provided power from both thermal and electrical sources. The coefficient s plays the role of an equivalence factor between them, to consider the difference on efficiencies between the two mechanical power sources.

$$H = P_{fuel} + s \cdot P_{echem} \qquad (3)$$

Consequently, the two terms on Equation 3 are viewed as costs, while s is a weighting factor for the electrochemical power. If s has a high value, an increase on P_{echem} will lead to a more significant Hamiltonian increase, decreasing the chances of this power value to be the chosen one.

Therefore, the coefficient s can control how the energy distribution will be performed during the calculation. Since the model concerns a mild-hybrid vehicle, and since the driving cycle is previously known, s is optimized in a way that the SoC at the end of the cycle is the same as at the beginning of the cycle (except for the ZEV mode).

In order to apply the PMP, the values of the DoFs of each mode were discretised with values between their boundaries, as done for the TAPIoCA script. Then, H is calculated for each possible value and the set of DoFs values whose H is minimum is retained.

Degrees of freedom definition

As already discussed, each mode has a different number of DoFs. For the Simulink model, the parameters taken as degrees of freedom are not necessarily the same as the ones shown on Table 4. Table 5 presents the two first parameters selected as DoFs. Even though the mechanical transmission is also a parameter of influence, its values are only explained in the next section

Table 5: Degrees of Freedom for each mode

Mode	DoF 1	DoF 2
Conventional	-	-
Parallel	T_{MG1}	T_{MG2}
Series	T_{ICE}	N_{ICE}
ZEV	T_{MG2}	

Since the complexity of the Simulink model is higher compared to TAPIoCA, the level of discretisation of the DoFs has an important role on the results. Therefore, the study performed first was a sensitivity analysis on this level of discretisation.

Choice of transmission ratios

On the P1*/P4 architecture, mechanical components result in a reduction ratio along the power path. To run the simulation, these ratios must be defined *a priori*.

Rear final drive (FD_R): The rear final drive ratio was fixed to 4. That allows the mechanical transmission to have ratios values usually encountered in the market.

Mechanical transmission (MT): In respect with the vehicle requirements, CVT was considered a good match for this application. The transmission boundaries were chosen in a way that the ratio of the highest reduction ratio leads to a relation of vehicle/engine speed

Table 6: Steps of the electric powertrain optimization process

Step	Tunes Parameter	Criteria
1	Total Electric Power	Do Phase 1 and Phase 2 on series mode
-	**(Verification)**	Demanded battery power lower than minimum
2	Number of supercapacitor cells	ZEV cycle without surpassing P_{batt} peak
3	Battery Energy Capacity	ZEV cycle until 30 km
4	Minimum MG1 Torque	Minimum torque to start ICE
5	Maximum MG1 Torque	Minimum MG2 torque to do Phase 1 and 2 on series mode
6	Final MG1 Torque	Optimized correct fuel consumption with MG1 torque between boundaries

of 8km/h/1000rpm, for driveability purposes; and the lowest reduction ratio leads to an engine speed of 3000 rpm at a vehicle speed of 110 km/h, i.e. 36,67 km/h/1000rpm.

ICE/EM1/MT mechanical coupling: As discussed, the implementation of a coaxial motor was chosen, therefore the ratio between the ICE, MG1 and the manual transmission is 1.

Front final drive (FD_F): For the hybrid series driving mode, MG2 is the only positive torque source. This machine should at least be able to achieve the base speed, after which the maximum power output remains constant. Since the front final drive is the only ratio between the front wheels and MG2, its value is critical to define the operating points of the latter. However, this ratio cannot be too high to the point of resulting in a motor speed higher than 14000 rpm, which is its maximum speed, problem that can occur on parallel mode operation (speed up to 110 km/h). In a pre-study, a value of 11.8 for the FD_F was deemed suitable to respect the conditions mentioned before.

Phases of the Artemis cycle

Since the different modes have different performance depending on the driving conditions, the Artemis cycle was divided in four different phases to represent different scenarios, as shown on Figure 10.

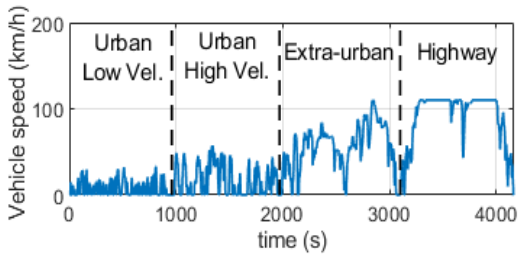

Figure 10: Four different phases of Artemis

Electric powertrain optimisation

Regarding the electric motors, even though the different power ranges for the vehicle to achieve the requirements were defined, these numbers should not be considered until the end of the design, due to reasons such as: powertrain and driveline losses, the fact that the mechanical power sources do not always provide their maximum power (since it is a function of speed), and the fact that some driving modes depend strongly on the power of a specific component. In addition, verifications of the battery power limit should also be performed, in order to verify if the supercapacitor is a required feature or if it is optional. Therefore, an optimization study was performed, whose steps are presented on Table 6. For the ICE, the 0.3 L of displacement was kept, since it already provides the power to achieve a 110 km/h velocity.

For the 4th step, the required MG1 torque to start the engine was calculated by implementing Equation 4, considering 1 bar of FMEP and the inertias, on a standalone Simulink model. This corresponds to the torque required to overcome friction and inertial forces for a start-up in less than 0.5s.

$$T_{MG1} - T_{FRICTION} = (J_{ICE} + J_{MG1}) \cdot \frac{d\omega_{ICE}}{dt} \quad (4)$$

Scenarios toward the optimisation of the powertrain

Sensitivity analysis

As explained earlier on, the different degrees of freedom of the hybrid powertrain are discretised, for the hybrid energy management system to calculate at each time step the available options and to find the optimal one. Therefore, the number of discretised steps has an influence on the calculation time as well as on the results, thus, a short sensitivity analysis has been conducted.

Figure 11 shows the results of an analysis conducted on the two degrees of freedom of the series mode. It can be seen that the relative variation becomes less than 1% for more than 8 steps of discretisation. For the rest of the study, a value of 10 is chosen, except when the gear box ratios are used as degree of freedom. In that case, in order to mimic closely the behaviour of a CVT, 20 discrete values are used.

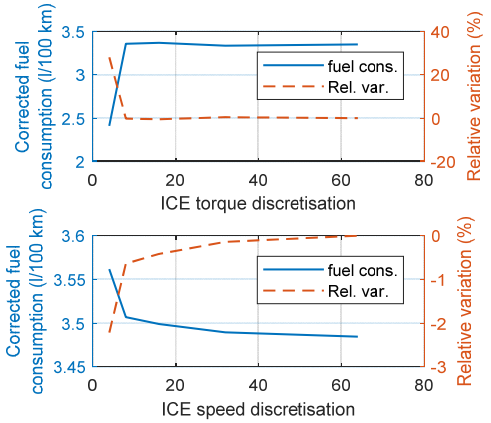

Figure 11: results of the sensitivity analysis - Series mode on the first two parts of the Artemis cycle

Powertrain optimisation

In that part, the main parameters of the architecture will be determined and optimised, according to the procedure described in Table 6. Results are presented below:

- Step 1: Electric Power required: 14 kW.

Verification: Battery Peak power in electric mode: 15 kW => impossible for the chosen type of battery (limited to 5 kW).

- Step 2: Supercapacitor: 9 cells in series, on 3 parallel lines (see *Hybrid energy storage* section).
- Step 3: Battery sizing: 13 cells in series and 21 cells in parallel (cell capacity: 3.2 Ah). Battery is described later. The pack is sized in order to be able to run 30 km without reaching the minimum SoC at 20%. Figure 12 illustrates this method with the last 30 km of the Artemis cycle (saturated at 70 km/h), but the test has also been made on the first 30 km (lower speeds but tougher accelerations).

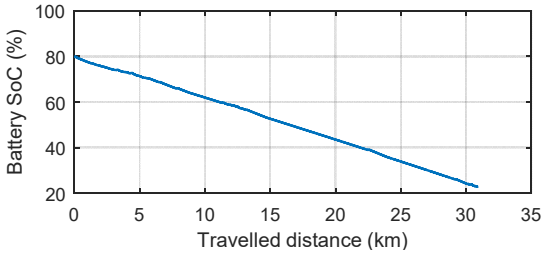

Figure 12: SoC evolution with travelled distance (ZEV mode, last 30 kms of the cycle)

- Step 4: Minimum MG1 torque required to start the engine: 7 Nm.
- Step 5: Maximum $T_{MG1,max} = 10\,Nm$. Above this value, the maximum torque of MG2 (at constant electric power) is too low for the vehicle to follow the first two phases of the cycle in series mode.
- Step 6: Optimal $T_{MG1,max} = 8\,Nm$. This value has been chosen between the two extreme values determined earlier. A short study with different values showed a very low influence on the final consumption.

Requirements validation

Maximum speed and 0-100 acceleration

Figure 13 shows that the vehicle fulfils the 0-100 km/h acceleration and the maximum speed requirements.

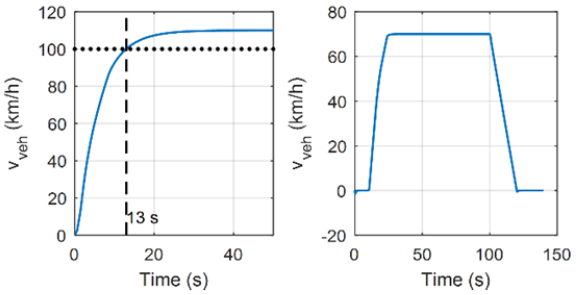

Figure 13: acceleration from 0 to 110 km/h (left, parallel mode) and test of maximum electric speed (right)

Maximum speed in electric mode

Figure 13 shows that the vehicle fulfils the requirement for maximum EV mode speed.

Stop and Start operation

Figure 14 illustrates the operation of the stop and start system: after 30 seconds of engine running, the ICE is shut off until the vehicle needs traction power. The first running phase (40 s – 120 s) lasts more than 30 seconds, therefore, as soon as the vehicle stops, the engine is switched off. The second running phase (150s – 170s) lasts only 20 s, therefore, the engine keeps running 10 s after the vehicle stop.

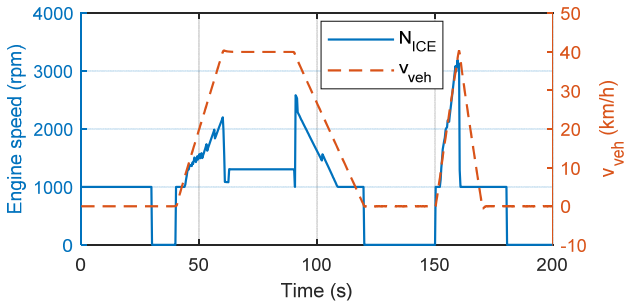

Figure 14: illustration of the Stop and Start system operation (conventional mode)

Electric motors peak power

Electric motors cannot work at their maximum power for long time. Overheating issues require that both motors should not operate at more than 70% of their maximum torque for more than 30 seconds. Table 7 shows the maximum durations spent over this limit for both machines.

Table 7: maximum duration over 70% of maximum torque (in seconds) for MG1 and MG2

	Parallel Mode (full cycle)	Electric Mode (phase 1 and 2)
MG1	3.3	4.2
MG2	5.7	6.0

Fuel consumption analysis

Best mode per phase

Figure 15

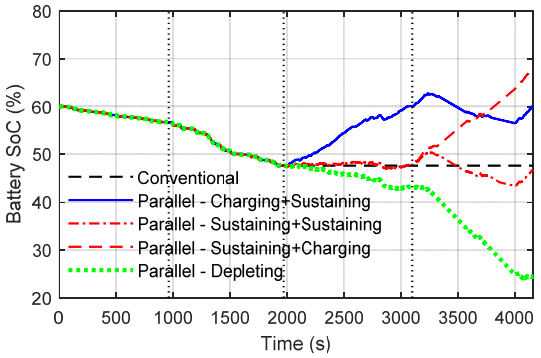

and Table 8 show the results of the simulations, in terms of fuel consumption, for the different modes, on the four phases of the Artemis cycle presented on Figure 10. In the first two phases, series and electric modes were considered, while in the last two ones, speeds are too high for these modes, therefore, conventional and parallel modes only are used.

Stop and start system, when used alone, offers significant improvement compared with non-micro hybrid system. As the stop and start system is used in parallel mode, this helps understanding which part of the consumption gains is due to the micro-hybrid

device. The stop and start system can bring up to 9% of fuel consumption gain in low speed phases.

Except during Phase 1, parallel mode is always the best hybrid mode and always more interesting than conventional operation.

At very low speeds (Phase 1), where the ICE is likely to work on low efficiency points in parallel and conventional applications, the series mode offers some energy savings. It can be used in that case, when the electric mode is not available.

Thanks to a higher efficiency, electric mode is significantly superior to the other ones when it can be used (i.e. when the speed is low enough and the battery SoC high enough).

Table 8: corrected fuel consumption for the different modes on the different phases

(l/100 km)	Conv.		Conv. + S&S		Parallel		Series		ZEV	
Phase 1	5,4	0%	4,9	9%	4,4	19%	4,2	23%	0,6	89%
Phase 2	4,1	0%	3,8	7%	3,1	24%	3,5	14%	0,7	82%
Phase 3	2,9	0%	2,9	1%	2,6	10%				
Phase 4	3,6	0%	3,6	0%	3,6	2%				
Average	**3,5**	**0%**	**3,4**	**2%**	**3,2**	**7%**	**3,7**		**0,7**	

Example of a driving scenario

In this scenario, the vehicle is assumed to start the Artemis cycle with a battery SoC at 60%. It is therefore possible to run in full electric mode in the first phases of the cycle (as the previous study showed that this mode was much more efficient than the other ones when available), during which the battery is depleted (see Figure 16). Then, 5 possibilities are studied:

- The vehicle switches in conventional mode for the rest of the cycle (black dashed line).
- The vehicle uses the parallel mode to recharge the battery up to 60% during the third phase and then the SoC is maintained during the last phase (blue line).
- The parallel mode is used to sustain the battery SoC until the end (red dashed and dotted line).
- The parallel mode is used to sustain the charge during the third phase and then recharges the battery during the last phase (red dashed line).
- The vehicle works in parallel mode until the end of the cycle while depleting the battery (green dotted line).

Figure 17 shows that, after a charge deplete due to electric mode, using the parallel mode to charge the battery (parallel mode is in fact the only available solution on phase 3 and 4) leads to a tight increase in fuel consumption compared to a switch to conventional mode. Energy consumption can be improved if the battery state is kept constant (manageable for a non Plug-In HEV). However, the most efficient is to use the remaining energy to assist the powertrain in highly power demanding phases. This last option requires the use of a PHEV, or an alternative way to quickly put energy inside the car, such as battery swap [10].

Hybrid energy storage system

As described previously, the battery voltage is set to 48 V. The peak powertrain power being about 14 kW, the current level is significant (approx. 290 A), hence leading to poor battery efficiency and premature ageing. Therefore, supercapacitors are added in parallel with the battery.

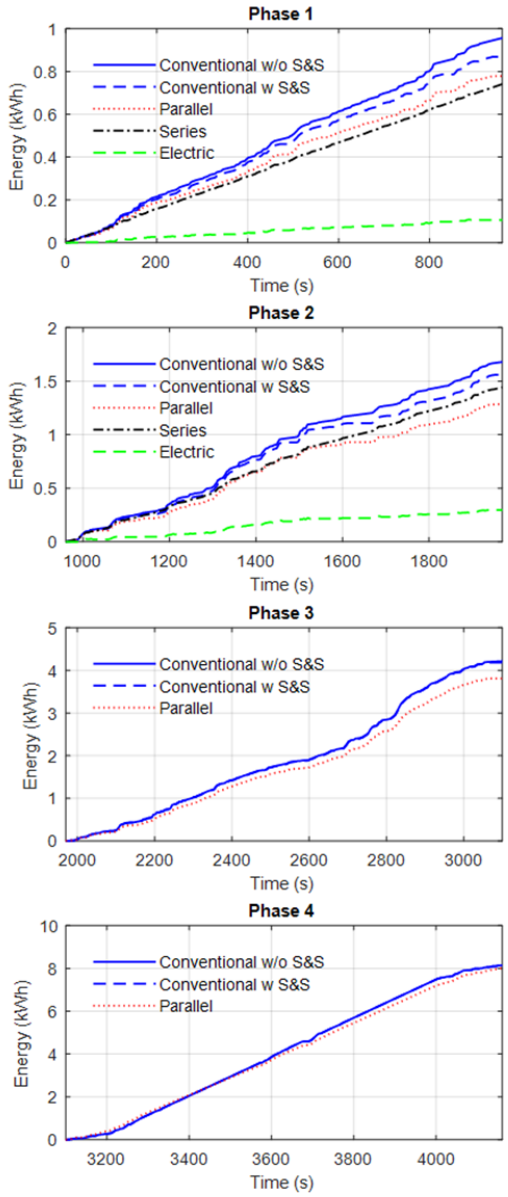

Figure 15: energy consumption on the different phases of Artemis for the 4 modes

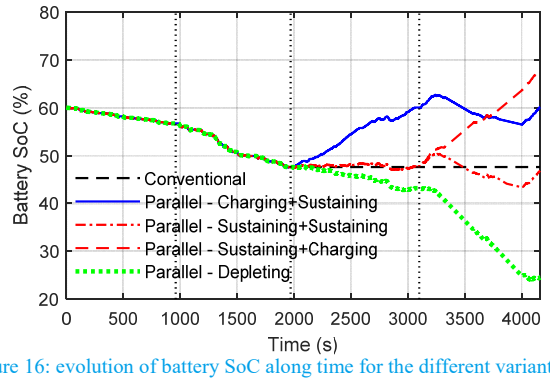

Figure 16: evolution of battery SoC along time for the different variants of Driving Scenario.

They are used as power source, providing the sharp power request, while the battery is used as energy source. The dynamic performances of the vehicle will not be lowered by this modification.

Supercapacitor description and integration

A supercapacitor is an electrical energy storage device, built similarly compare to a battery, but with a much higher power density and lower energy density [11]. Moreover, it has an outstanding life span and can withstand a high number of discharge and recharge cycles. Hence, it is used as power buffer, providing peak current asked by the powertrain while the battery is kept as main energy source. A DC/DC converter (see Figure 8) is used in order to adapt the supercapacitor voltage which is decreasing linearly with the depth of discharge.

The supercapacitor characteristics are taken from [12] and used in the simulation to build the desired hybrid energy storage system, combining 3 legs of 9 cells (27 cells) to reach a total capacity of 42 Wh.

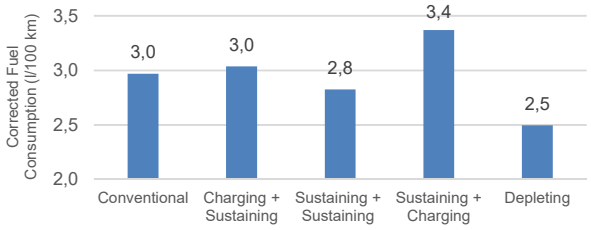

Figure 17: corrected fuel consumption for the different variants of Scenario 1

Energy management strategy

It is essential to restrict the battery operating range to maximise its effectiveness and lifetime. When electric power demand is higher than the battery threshold, the rest of the power is provided by the supercapacitors (transient driving phases).

On Figure 19, profile of the retained battery efficiency against depth

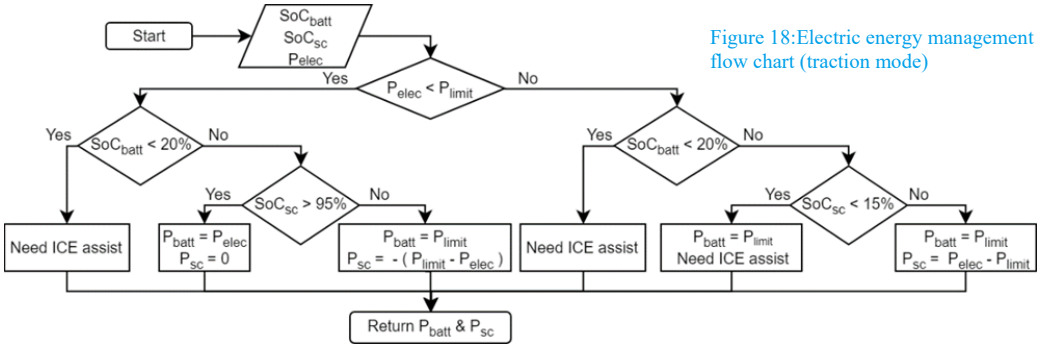

Figure 18:Electric energy management flow chart (traction mode)

of discharge evolution are shown. It can be observed that a maximal discharge current of 1.5C, appears as a good trade-off between electric power and moderate losses. According to the battery pack characteristics considered, this value of current corresponds to a maximal power of 5 kW. The power requirement study established that this figure was more than enough to fulfil the ZEV top speed 70 km/h requirement.

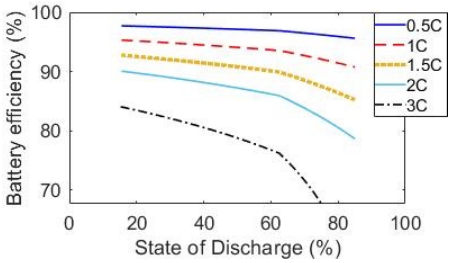

Figure 19: Battery maximum power determination

Figure 18 presents the principle of the power repartition between the two energy sources during traction mode. Based on the supercapacitor and battery State of Charges (SoC) as well as the level of power requested (P_{elec}>0), the different energy flows are identified, and the levels of power calculated. Typically, the battery supplies all the power up to the defined limit (P_{limit}: 5 kW). Then, the supercapacitors take over to assist the battery. The SoC ranges of battery and supercapacitor are restricted to enhance efficiency and ensure safety. The previous reasoning works similarly during generator phases.

Results and benefits of the designed system

As explained previously, the supercapacitors allow to reduce the electrical load on the battery. Figure 20a) shows the battery power during the Artemis phase 1 and 2 for two configurations: with and without supercapacitors in ZEV mode. The described power distribution strategy enables to limit the maximum limit current of the battery when supercapacitors are added in parallel. Moreover, the supercapacitor SoC during the cycle is represented Figure 20b). Each sharp decrease of the SoC corresponds to a limitation of the battery power and hence an assist by the supercapacitor. During these low speed phases, the supercapacitor SoC never depletes below 70% which ensures a sufficient power reserve for heavy acceleration (not met during homologation cycle).

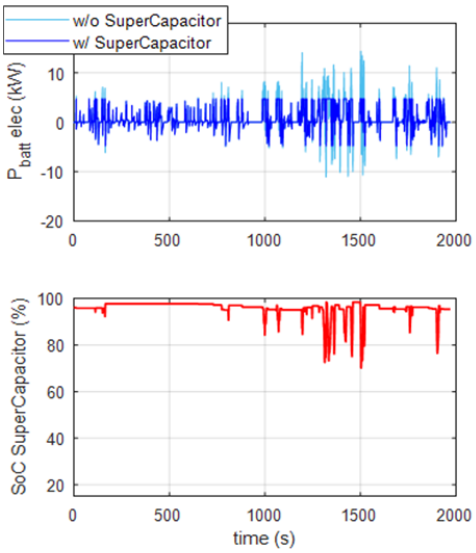

Figure 20: a) battery power b) supercapacitor SoC in ZEV mode on Artemis phase 1 and 2

Battery cooling estimation

During their operation, batteries heat up because of chemical reactions and internal resistance, of the battery itself or its busbars. In the battery model, the internal resistance only is considered, and the losses will be calculated by measuring the difference between electric and electrochemical battery power.

The battery temperature is calculated using the following formulae:

$$m_{batt}.cp.\frac{dT_{batt}}{dt} = P_{batt} - P_{exch} \quad (4)$$

$$P_{exch} = h.A.(T_{batt} - T_{amb}) \quad (5)$$

$$P_{batt} = |P_{elec} - P_{electrochem}| \quad (6)$$

As this is just an estimation of the battery heating, approximated values will be used, with:

$cp \approx 800\, J.kg^{-1}.K^{-1}$ [13], [14]

The heat exchange area is supposed to be equal to the lateral area of the cylindrical cells.

The parallel case has been used on a complete cycle, as it is supposed to be the toughest case for the battery.

Results are presented on Figure 21Figure 21. Lithium-ion batteries optimal operating temperatures are between 10 and 35 °C [15], therefore, this graph shows that the minimum coefficient of convection h that could lead to acceptable battery heating is around $200\, W.m^{-2}.K^{-1}$. This value corresponds to a forced air-cooling usual value.

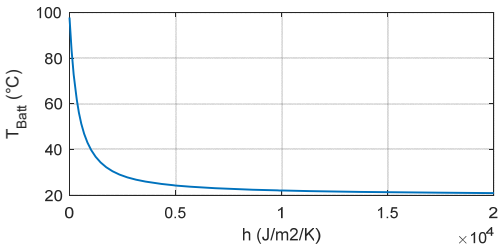

Figure 21: thermal study of the battery and the supercapacitor (ambiant temperature: 20°C)

Electro-mechanical integration

Mechanical parts

Engine & ATS: A 0.3 L gasoline engine is mounted on the vehicle with a close coupled three-way catalytic converter to reduce emissions and comply with legislation. Moreover, in a near future, the 48V system of the vehicle could be extended to refine the engine. Many components could be electrified (water pump, AC compressor, oil pump, …) reducing considerably the powertrain weight and CO_2 emissions (up to 4% in WLTC) [16].

CVT & FD: A continuously variable transmission (CVT) is selected to match the gearbox requirements. It allows to have an uninterrupted ratio between two extreme values. The control of the CVT is quite simple and therefore suitable for a hybrid powertrain. The maximum torque being 60.5 Nm, this solution will stay relatively cheap and compact (low centre distance) and have a decent efficiency, compare to automatic or double clutch transmissions. Hence, such a system, which is already implemented on small cars or powerful 2-wheelers (with centrifugal actuation), represents a good trade-off.

The two final drives are gear meshed reducer. It enables high power transmission, low cost and good efficiency.

Clutch: Two clutches are needed to couple the different elements of the rear axle: one between the ICE and the EM and another one between the latter and the gearbox (Figure 8). The first one is only used as ON/OFF clutch to connect two shafts when standstill. On another hand, the second engages two shafts when rotating, and especially connects the ICE to the wheels. Therefore, the first clutch is a dog clutch, enabling low complexity, whereas the second one is a friction cutch, enabling ICE connection. Both are electrically actuated and controlled by the ECU.

Electrical parts

eMOT: Amongst all the existing electric machine, the permanent magnet synchronous machines (PMSM) are currently the most used in HEV. Indeed, they have a high torque-to-mass and power-to-mass ratios combined with good efficiency. Even if the presence of rare earth makes it expensive and sensitive to supply, the power levels required for the designed ultralight vehicle are only 4.1 and 9.9 kW which reduce the impact of such issue [9].

Power Electronics (PE): Various types of PE are needed in the powertrain to control the electric energy supplied. First, inverters are integrated to transform the DC power from the energy storage system into AC power which is fed to the electric machines thanks to pulse width modulation (PWM) method. Secondly, the voltage levels being different for the main battery, the supercapacitors and the auxiliary battery, two DC/DC converters are added. One is used to increase the supercapacitor voltage to 48 V to match the main battery, and the other to adapt the voltage from 48 to 12 V between the two batteries.

Supercapacitors (SC): As described earlier, the supercapacitors added to form a hybrid energy storage system are taken from [12]. They are selected for their very high power density enabling to play the role of power buffer.

Battery: The general requirements sought for the battery pack are: a high energy density (light battery pack), a high number of life cycles (longevity), and safety (prevention of thermal runaway for instance). Of course, the cost and maturity of the technology are paramount. For these reasons, lithium-ion batteries (Cobalt/Carbon electrodes) are a very good fit for this application [17]. It is to note that BMS and cooling system are mandatory for this type of cells and should be accounted for when assessing the total cost and weight/volume of the battery system.

The choice of using 48 V for the electric system, and a quite high electric powertrain power means that the current flowing through the battery pack is relatively high. Supercapacitors help reducing power peaks, but a sustainable current of 105 A has to flow though the battery without causing significant losses or damages. Putting this in perspective with the requirements of the vehicle means that the number of cells as well as the cost have to be as low as possible. In this respect, two models of cells corresponding to high energy density (NCR18650B) and high power density (UR18650RX) have been compared. Their relative characteristics have been summarized Figure 22:

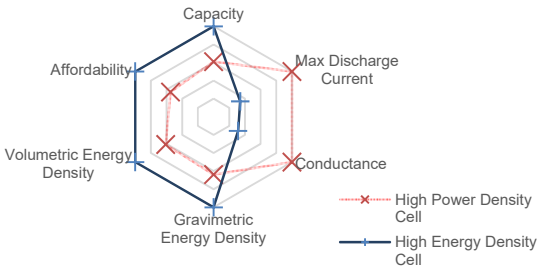

Figure 22: Relative performances of high power/energy density cells.

There, the conductance reflects the inverse of the internal resistance, i.e. the tendency of the cell not to suffer Joule effect. It is clearly seen that the high power density cell is behind the high energy density cell in most aspects except the current it can admit. When sizing the battery pack with high power density cells, 50% more legs in parallel have to be added compared to one made of high energy density cells in order to keep the same energy capacity. Even with the extra power to the battery, the penalty in weight, volume and cost is not worth it when supercapacitors could be used in a far less number to make up for this power difference.

Packaging and cost constraints

The major challenges when designing an ultralight urban HEV are the mass and volume. The hybrid powertrain should fit in the car,

without compromising the passenger compartment and keeping a good mass reparation on the chassis for drivability. Moreover, in a context of price war between the OEMs, the cost constraint is paramount when designing a new vehicle. Therefore, every component must be sized effectively, fulfilling its mission without over quality.

The mass and cost of the chosen powertrain elements are estimated and summarised in Table 9. These values are based on the case study input assumptions for specifications, component datasheets, scientific papers and other assumptions.

The battery cell gravimetric and volumetric energy density are respectively 243 Wh/kg and 676 Wh/L (ref pana [1]). The ones of supercapacitors are 10 Wh/kg and 18 Wh/L [12]. It is assumed that all the elements surrounding the cells (BMS, cooling system, etc.), represents an extra 70% weight and volume. Hence, it leads to a global pack of 28 kg and 8 L. This good performance is the result of combining high energy density battery cells with high power density supercapacitors.

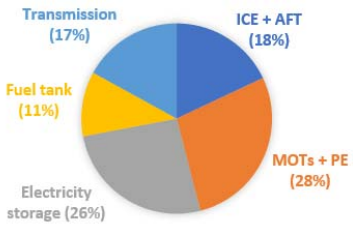

Figure 23: Powertrain mass repartition

The powertrain total mass (repartition shown Figure 23) is estimated around 109 kg and hence it represents a fourth of the vehicle curb weight. This value is in the order of magnitude of a usual HEV. In addition, the volume of the powertrain is minimised using the hybrid energy storage system and a coaxial electric motor MG1. The two electric motors are also spread on the different axles to reduce packaging issue and unbalanced masses. Finally, the powertrain cost is kept under €1400. Assuming a target vehicle at €7000, it represents around 20% of the total cost.

Therefore, the previous considerations regarding the packaging and cost give credibility to the designed solution. The developed powertrain is compliant with the initial objectives which aim to design a compact HEV powertrain under high cost constraint.

Table 9: Mass and cost summary estimation

	Mass (kg)	Cost (€)
ICE & AFT	20[(1)]	368 [18]
eMOTs & PE	31[(1)]	223[(5)] [19]
Elec. Storage	28 [20] [12]	565[(4)] [21] [22]
Fuel Tank	12[(2)(3)]	20[(3)]
Transmission	18[(6)] [23]	171[(6)] [24]
Total	**109**	**1347**

[(1)] Case study initial assumptions; [(2)] Based on fuel consumption and total range; [(3)]Estimated values; [(4)] Assuming 176$/kWh for the battery pack and 2,500$/kWh for the supercapacitor; [(5)] According to REF[4] the costs of PMSM and PE are respectively 12.9€/kW and 3€/kW; [(6)] Shafts, clutches and final drives values estimated

Connectivity

The digital revolution impacts all the sectors and the industry 4.0 is becoming a reality. The automotive sphere is not spared, and car makers have to move toward more connectivity to face current major challenges such as reducing road congestion or improving fuel efficiency and safety. Besides, connectivity could play a key role to enhance the user experience trough more interactions with vehicle occupants.

Toward a more pleasant trip

The user experience in tomorrow's vehicles will be completely reshaped and adapted to new driver's expectations. The consulting firm McKinsey & Company has defined the C^3X framework which identifies five levels of car connectivity. It goes from the simple driver alert to a complete virtual chauffeur which knows user preferences and traffic information in real time. But this feature needs a tremendous amount of data from vehicles to process it and turn it into a valuable item. These vehicle data could worth up to $750 billion by 2030 [25] and become the major lever for a better understanding of customer needs.

In the frame of ultra-light urban vehicles, the connectivity could also be an effective way to tackle road congestion and reduce daily commuting time. The vehicle to vehicle or vehicle to infrastructure communications (grouped as V2X communications) are valuable players to offer a range of benefits in terms of road safety, traffic efficiency and driver convenience [26]. Associated with appropriate infrastructures, such as dedicated lines and smaller parking slots, it could strengthen the credibility of using an ultra-compact HEV in dense areas.

Toward a more efficient trip

The European Automobile Manufacturers Association identified the main options to reduce vehicles CO_2 emissions among them driver behaviour and connected technologies play a significant role [27].

Based on car sensing data, it is possible to classify driver usage into different profiles [28] and use it as reference to help the driver adopting an eco-driving style. By training the driver or instantaneous in-vehicle feedback thanks to ADAS, the CO_2 benefits can reach 15% according to [27]. Combined with a user-friendly interface, the real time driver coaching could be part of tomorrow's mobility, helping the driver to manage effectively the available power.

Moreover, the energy management system (EMS) of the HEV can be improved thanks to intelligent transport systems. A predictive strategy based on a learning process can anticipate the driver journey and adopt the most efficient EMS accordingly. The system records the vehicle data and adapts its strategy as a function of each use. It has been proved that the daily commuting trips on weekdays could be predicted with a success of 84% [29], enabling an optimal EMS solution reducing tremendously the fuel consumption [30]. It is also possible to go further and directly ask the driver to indicate its destination. In this way, the optimal path is found using V2X communications and the associated optimal EMS adopted.

Practically, it means using an online Pontryagin's Minimum Principle based on instantaneous driver request [9], opposed to the offline

method, based on a driving cycle, defined earlier. The additional information (e.g. planned trip, road conditions, etc.) are used to estimate effectively the coefficient s to minimise energy consumption, enabling approximately 10% CO_2 reduction [27].

Finally, connectivity could be used to enhance both fuel and traffic efficiency with a redesigned user experience. It needs a strong cooperation between automotive and software sectors, combined with improved infrastructures and good public acceptance. In that conditions, it could become the key point for tomorrow's mobility.

Summary/Conclusions

In this paper, a hybrid vehicle architecture adapted to an ultra-light vehicle is designed and its performances are evaluated. The three different considered architectures are compared using the developed in-house calculation tools and practicality analysis. Between them, the P1*/P4 architecture is chosen for the ability to split up the powertrain between the front and rear axle, increasing the architecture flexibility. A 48V power network is taken for its low cost and high simplicity, and a supercapacitor is implemented to support the battery and avoid the need of an expensive powerful battery. An estimation of the consumption for the vehicle is calculated on the Artemis cycle for different outcomes, and low values are observed. Finally, an analysis on connectivity technologies shows that techniques, such as V2X, can further improve the vehicle efficiency.

References

1. Federal Highway Administration, "Average Vehicle Occupancy Factors for Computing Travel Time Reliability Measures and Total Peak Hour Excessive Delay Metrics," no. April, pp. 1–8, 2018.

2. D. Fiorello, A. Martino, L. Zani, P. Christidis, and E. Navajas-cawood, "Mobility data across the EU 28 member states : results from an extensive CAWI survey," Transp. Res. Procedia, vol. 14, pp. 1104–1113, 2016.

3. J. Mortal, "Optimisation of Electric Drive Units for Low Speed Electric Vehicles," 2019.

4. M. Forissier, "L'electrification des vehicules : pas si simple !," 2019.

5. R. Rajamani, Vehicle Dynamics and Control, Springer. 2006.

6. G. Lino and A. Sciarretta, Vehicle Propulsion Systems, Springer. 2007.

7. Green Car Congress, "Bosch introduces new 48V Li-ion pack for mild-hybrids; production in 2018," 2017. Online.. Available: https://www.greencarcongress.com/2017/10/20171019-bosch.html.

8. L. Guzzella and A. Amstutz, "CAE Tools for Quasi-Static Modeling and Optimization of Hybrid Powertrains," vol. 48, no. 6, pp. 1762–1769, 1999.

9. F. Badin, Hybrid Vehicles, IFPEN. TECHNIP, 2013.

10. B. Subirana, M. Puig, and S. Sarma, "Can small smart swappable battery EVs outperform gas powertrain economics?," IEEE Conf. Intell. Transp. Syst. Proceedings, ITSC, vol. 2018-March, no. Saovapakhiran 2012, pp. 1–6, 2018.

11. A. Burke, "Chapitre 39: Electro chemical capacitors," in Linden's Handbook of Batteries (Fourth Edition), T. Reddy, Ed. McGraw-Hill, 2011.

12. A. Burke and H. Zhao, "Applications of Supercapacitors in Electric and Hybrid Vehicles," 2015 IEEE 82nd Veh. Technol. Conf., no. April, pp. 1–15, 2015.

13. M. Muratori, "Thermal Characterization of Lithium-Ion Battery Cell," Politecnico Di Milano, 2009.

14. H. Maleki, "Thermal Properties of Lithium-Ion Battery and Components," J. Electrochem. Soc., vol. 146, no. 3, p. 947, 1999.

15. J. Warner, "Lithium-Ion and Other Cell Chemistries," in The Handbook of Lithium-Ion Battery Pack Design, no. Cid, 2015, pp. 65–89.

16. H. Sorger, "The Tailored Engine & Powertrain for 48V," in Comprehensive Solutions for Optimum Efficiency and Cost, 2018.

17. Panasonic, "Panasonic overview lithium-ion batteries," 2007.

18. R. Kochhan, S. Fuchs, B. Reuter, P. Burda, S. Matz, and M. Lienkamp, "An Overview of Costs for Vehicle Components, Fuels and Greenhouse Gas Emissions," ResearchGate, no. February, pp. 1–26, 2017.

19. M. Fries et al., "Optimization of hybrid electric drive system components in long-haul vehicles for the evaluation of customer requirements," Proc. Int. Conf. Power Electron. Drive Syst., vol. 2017-Decem, no. December, pp. 1141–1146, 2018.

20. Panasonic, "Panasonic NCR18650B," Data sheet, no. 469, p. 2, 2012.

21. L. Goldie-Scot, "A behind the scenes take on lithium-ion battery prices," BloonbergNEF, 2019. .

22. A. Burke, "Energy Storage with Batteries and Supercapacitors in vehicle applications," Univ. California-Davis Inst. Transp. Stud., no. Decenber, 2017.

23. F. Van Der Sluis, S. Yildiz, A. Brandsma, P. Veltmans, M. Kunze, and B. T. T. B. V, "The CVT Pushbelt reinvented for Future Compact and Efficient Powertrains," no. September, 2016.

24. N. R. Council, Cost, Effectiveness, and Deployment of Fuel Economy Technologies for Light-Duty Vehicles. Washington, DC: The National Academies Press, 2015.

25. M. Bertoncello, A. Husain, and T. Möller, "Setting the framework for car connectivity and user experience," McKinsey, 2018. .

26. "The V2X (Vehicle-to-Everything) Communications Ecosystem: 2019 – 2030 – Opportunities, Challenges, Strategies & Forecasts," SNS Telecom & IT, 2019. .

27. "Reducing CO2 emissions from passenger cars and light commercial vehicles post-2020," Eur. Automob. Manuf. Assoc., no. May, 2016.

28. C. Barreto, A. M. P. Canuto, and I. Silva, "A Machine Learning Approach Based on Automotive Engine Data Clustering A Machine Learning Approach Based on Automotive Engine Data Clustering for Driver Usage Profiling Classification," no. October, 2018.

29. L. Joud, “Stratégie intelligente de gestion du système énergétique global d’un véhicule hybride,” École doctorale Sciences pour l’ingénieur et microtechniques (Besançon ; Dijon ; Belfort), 2018.

30. Q. Gong, S. Member, Y. Li, and Z. Peng, “Trip-Based Optimal Power Management of Plug-in Hybrid Electric Vehicles,” vol. 57, no. 6, pp. 3393–3401, 2008.

Contact Information

Dr.-Ing. Ouafae EL GANAOUI-MOURLAN: ouafae.el-ganaoui-mourlan@ifpen.fr

Definitions/Abbreviations

ZEV	Zero Emission Vehicle
$v_{max_{iZE}}$	Maximum speed in Zero Emission mode
DoF	Degree of Freedom
CVT	Continuously Variable Transimission
FD	Final Drive
H	Hamiltonian
V2X	Vehicle to everything
PMSM	Permanent Magnet Synchronous Motor
AFT	After Treatment System
PE	Power Electronics
GHG	GreenHouse Gas
LSEV	Low Speed Electric Vehicle
TCO	Total Cost of Ownership
ICE	Internal Combustion Engine
EM	Electric Machine
ECU	Electronic Control Unit
HEV	Hybrid Electric Vehicle
BMS	Battery Management System